Analytica Chimica Acta 1337 (2025) 343568

Contents lists available at ScienceDirect

Analytica Chimica Acta

journal homepage: www.elsevier.com/locate/aca

Determination of alkali metal elements in solid biomass fuel by laser-induced breakdown spectroscopy: Analysis and reduction of chemical matrix effects

Chengjun Li [a,b], Zhimin Lu [a,b,**], Jinzheng Chen [a,b], Ziyu Yu [a,b], Qi Yang [a,b],
Huaiqing Qin [a,b], Xiwen Xing [c], Qingxiang Ma [d], Shunchun Yao [a,b,*]

[a] School of Electric Power Engineering, South China University of Technology, Guangzhou, Guangdong, 510641, China
[b] Guangdong Province Key Laboratory of Efficient and Clean Energy Utilization, Guangzhou, Guangdong, 510641, China
[c] College of Life Science and Technology, Jinan University, 510632, Guangzhou, China
[d] State Key Laboratory of High-Efficiency Utilization of Coal and Green Chemical Engineering, Ningxia University, Yinchuan, Ningxia, 750021, China

HIGHLIGHTS

- The matrix effects caused by chemical properties in the measurement of alkali metals in biomass during LIBS are presented.
- Analysis elemental forms and biomass components effect on the spectral response and calibration curves.
- The accuracy of K content predictions for real biomass fuels is improved by correcting chemical matrix effects.

GRAPHICAL ABSTRACT

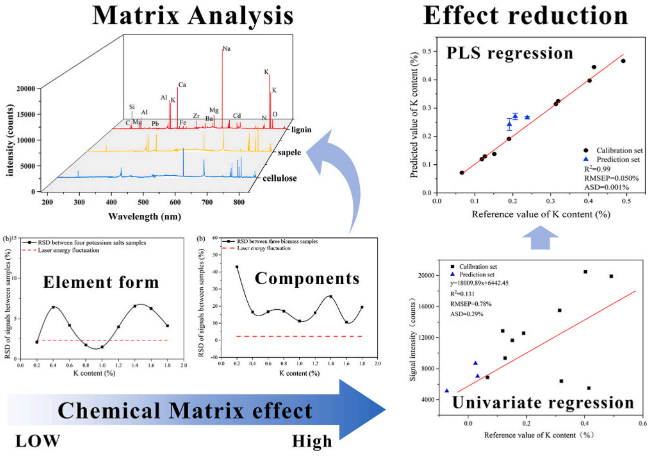

ARTICLE INFO

Handling Editor: Xiu-Ping Yan

Keywords:
Laser-induced breakdown spectroscopy
Chemical matrix effect
Biomass
Potassium
Calibration curves

ABSTRACT

Background: Rapid and accurate detection of the biomass potassium (K) content in biomass is crucial for mitigating ash deposition and fouling issues in biomass fuel combustion processes. Laser-induced breakdown spectroscopy (LIBS) offers a promising approach for rapid analysis of biomass elemental. However, the accuracy of LIBS detection is susceptible to chemical matrix effects. Particularly in the case of biomass, characterized by its complex composition, the absence of pertinent studies on effect mechanisms impedes the enhancement of analytical accuracy.

---

* Corresponding author. School of Electric Power Engineering, South China University of Technology, Guangzhou, Guangdong, 510641, China.
** Corresponding author. School of Electric Power Engineering, South China University of Technology, Guangzhou, Guangdong, 510641, China
E-mail address: epscyao@scut.edu.cn (S. Yao).

https://doi.org/10.1016/j.aca.2024.343568
Received 24 April 2024; Received in revised form 6 November 2024; Accepted 18 December 2024
Available online 19 December 2024

Results: In this study, we investigated and compared two types of matrix effects related to chemical properties in biomass samples (analyte forms and matrix composition). Firstly, the inconsistency of K spectral response among different chemical properties samples and the performance of univariate models were analyzed. The results indicate that, compared to the chemical forms, differences in composition are the dominant factor of chemical matrix effects. Moreover, the compositional content of biomass samples is analyzed to correlate the matrix effect in LIBS measurements to a chemical property of the specimen. It is indicated that differences in volatile and ash content may lead to variations in the plasma excitation process, resulting in distinct spectra. Finally, a knowledge-based regression approach was employed to attenuate chemical matrix effects, the main influencing factors identified were analyzed as a priori knowledge for variable selection and inputting them into a partial least squares model. And 13 real solid biomass fuels were measured, resulting in root mean square error of prediction (RMSEP), $R^{2,}$ and average standard deviation (ASD) of 0.99, 0.050 %, and 0.001 %, respectively.

Significance: This study investigated the influence of matrix effects related to biomass chemical properties on LIBS measurements, achieving rapid measurement of K. It promotes the application of LIBS in solid fuels and provides a methodological reference for LIBS analysis of complex matrix materials.

1. Introduction

Biomass as a renewable and zero-carbon energy source has garnered worldwide attention due to escalating environmental and energy concerns. It is primarily utilized as an alternative to fossil fuels in the form of solid fuels for firing and co-firing in power plants to generate electricity [1]. However, ash-related problems caused by alkali metal elements in biomass, especially potassium (K), pose significant obstacles to the combustion of biomass fuels [2]. The combustion and char of K-rich biomass release high concentrations of K compounds. These products can cause issues such as ash deposition on the fired surface [3] and slagging on the superheater [4], frequently resulting in unscheduled shutdown of the entire power plant. To control ash-related generation products and ensure the safe and efficient operation of power plants, rapidly determining K content in biomass fuels is therefore crucial.

Currently widely employed techniques for rapid elemental measurement in biomass fuels include inductively coupled plasma optical emission spectrometer (ICP-OES) [5], mass spectrometry [6], and X-ray fluorescence spectrometry (XRF) [7]. These methods involve several sample preparation steps and complex operation processes, demanding several hours to complete a determination, which is not suitable for industrial field applications. By comparison, laser-induced breakdown spectroscopy (LIBS) is an analytical spectroscopy technology with many attractive characteristics of no or simple sample pretreatment, rapid and simultaneous multi-element analysis, and in-situ measurements [8,9]. The application of LIBS in biomass fields has been initially researched [10], such as characterizing the release of K during the pyrolysis process of biomass, determination of calorific value, and proximate analysis in biomass fuels. For the former, a calibration curve and linear expression relating K concentration to the spectral line intensity at 766.49 nm are established through LIBS measurements of known concentration Potassium chloride solutions that had been fog generated from an ultrasonic vaporizer in a high-temperature experimental environment [11]. This expression is then used to calculate the release of K during the pyrolysis of biomass, which focuses on the characterization of changes in K release and does not lead to an accurate measurement of potassium levels[12–14]. Additionally, concerning the latter, investigations have been conducted on the correlation between indicators of real biomass fuel properties and the emission lines of key elements[15–17]. The effect of biomass pellet forming parameters on LIBS measurements was analyzed, and build prediction models for the quality indexes of biomass pellets [18,19]. Despite these advancements, as far as our knowledge extends, there has been no further research on the measurement of potassium content in biomass. This is possibly attributed to the matrix effects arising from the complex composition of biomass and the occurrence form of elements.

Fundamentally, matrix effects in LIBS refer to the different laser ablation behaviors and plasma evolution processes caused by variations in the physical and chemical properties of the sample, leading to different spectra [20]. Among these, matrix effects related to the chemical properties of materials are the predominant factors. To address chemical matrix effects, methods such as the use of additives [21], introduction of additional measurement parameters [22], and integration with other spectroscopic techniques [23] have been proposed. These approaches are primarily laboratory-based and offer limited effectiveness, while also increasing the complexity of sample preparation. Additionally, they require additional sophisticated instrumentation, making them unsuitable for industrial applications. Machine learning and chemometric methods offer effective means to address matrix effects. The use of nonlinear models [24] or spectral knowledge-based regressions [25] to attenuate the effects of complex matrices, and separate regressions using matrix matching [26], can be in improving quantitative accuracy. Nevertheless, these methods are heuristic, and a clear depiction of the impact patterns of chemical matrix effects in biomass would be advantageous for elements quantitative in biomass analysis. Yet, a clear theoretical explanation of its impact on LIBS signals is still lacking. There were many inconsistent conclusions in the literature. Sánchez-Esteva et al. [27] it was found that for the same phosphorus (P) content in the LIBS soil analysis, samples in the form of hydroxyapatite had lower P 213.6 nm spectral intensities than Fe (III) phosphate and potassium phosphate. Dong et al. [28] observed in coal particles that, with the same added amount of K, the spectral intensity emitted by KCl samples was more substantial than that of samples with added K_2CO_3. Conversely, other research indicates that differences in the content of non-target elements can lead to chemical matrix effects. For example [29], investigated the chemical matrix effect in industrial steel samples, revealing a significant reduction in overall LIBS spectral intensity with an increase in Si element content ($\geq$2 wt%) [30]. improved the accuracy of quantitative Cr in biochar by establishing a classification regression model. The results indicated that the major elements (C, H) content in biochar were the key factors contributing to the chemical matrix effect. These studies have solely focused on individual chemical matrix effect influencing factors in LIBS measurements. However, in the case of complex matrices, particularly biomass, affected by various factors.

Therefore, evaluating matrix effects associated with the chemical properties of biomass and conducting quantitative analysis of K within biomass represents a crucial research gap that needs to be addressed. This study contained mainly two parts. First, design an experiment to investigate and compare the chemical matrix effects induced by biomass composition, and chemical forms of potassium when LIBS measurements. Second, considering the predominant factors of matrix effects, establishing a quantitative model for K content in real biomass fuels has led to improved accuracy of quantification compared to calibration curves.

2. Materials and methods

2.1. Biomass sample

The experiment was divided into two parts to explore and compare the effects of differences in K chemical form and biomass sample composition on LIBS measurements, respectively. Both experiments utilize the impregnation method to generate specific types of samples with comparable K content, and the sample configuration information is shown in Table 1. Specifically, K element in biomass generally exists in the form of water-soluble potassium salts [2], such as KCl, K_2CO_3, K_2SO_4, and KNO_3, representing different chemical forms of K. Biomass is composed of lignin, cellulose, and hemicellulose in specific proportions [31], representing different composition of biomass. However, the complex structure of hemicellulose makes the impregnation process difficult to realize, so the raw biomass material Sapele is used as a substitute. Four different types of samples with varying chemical forms of K are obtained by impregnating the four potassium salts into cellulose samples. Additionally, KCl is impregnated into the three types mentioned above of samples to create three different biomass samples with distinct compositions.

Cellulose, Lignin, and Sapele have been used as original materials (Shanghai Macklin Biochemical Co., Ltd). The results of the proximate analysis of the three samples were determined according to the Chinese National Standard GB/T 212–2008 using chemical analysis methods are summarized in Table 2. Experimental Sample preparation included three steps: water washing, impregnating, and pressing. Firstly, washing with water is performed to remove different chemical forms of K from the original samples effectively [32]. Prepare 160g each of Cellulose, Lignin, and Sapele materials, which are dissolved in deionized water at a solid-liquid ratio of 40 g/L, undergoing room temperature stirring for washing. The water is changed every 12 h, with two water changes for each sample. The cleaned samples are placed in a 60 °C drying oven until a constant weight is achieved, serving as blank samples. The EDS (X-MaxN20EDS, Oxford Nanopore Technologies, England) is then utilized to determine the K content change before and after washing. The results in Table 3 indicate that water washing has removed most of the different chemical forms of K in biomass, but there is still a tiny amount of residue in lignin samples. To mitigate the influence of residual potassium in the samples after washing on spectral analysis, we will deduct the net intensity values of the spectral lines of K in the blank matrix during subsequent analysis. Subsequently, specific samples are obtained through impregnation. Four types of potassium salts, KCl, K_2CO_3, K_2SO_4, and KNO_3, were prepared for impregnation in 9 increments on a 0.2 % gradient (0.2%–1.8 %). 10g of blank sample and the corresponding concentration of required crystalline salt are placed in a beaker, filled with water to the liquid level aligned with the 80 ml scale, and put on a magnetic stirrer. After stirring at room temperature for 4 h, it is dried in a 45 °C oven for 48 h. Then, 1.50g of dried sample is weighed and placed in an automatic particle press (Pike Technologies Crusher), pressed for 2 min under a pressure of 9 tons, resulting in granular samples with a diameter of 24 mm and a thickness of 2 mm. This step aims to maximize the homogeneity of LIBS analysis samples, thereby minimizing the impact of physical matrix effects. Finally, 63 samples of seven different types were prepared, with K content ranging from 0.2 % to 1.8 %.

Table 1
Details on sample preparation.

Experimental parameters	Matrix composition experiment	K form experiment
Biomass	Lignin, Cellulose, Sapele	Cellulose
K impregnation content (%)	0.2, 0.4, 0.6, 0.8, 1.0, 1.2, 1.4, 1.6, 1.8	
K impregnation form	KCl	KCl, K_2CO_3, K_2SO_4, KNO_3

Table 2
Proximate analysis of three different types of samples.

Proximate analysis (%, ad)	Lignin sample	Cellulose sample	Sapele sample
Volatile	60.43	86.46	80.02
Ash	14.75	6.24	4.53
Fixed Carbon	20.93	4.87	11.92
Moisture	3.89	2.43	3.53

Table 3
Potassium content (atomic percent) in the three samples before and after water washing as measured by EDS.

Biomass sample	Potassium content before washing (%)	Potassium content after washing (%)
Cellulose	0.00	0.00
Sapele	0.01	0.00
Lignin	0.24	0.10

In addition, 13 solid biomass fuel samples were collected from different power plants in southern China, mainly in the form of 6–8 mm pellets. The K content was determined according to the Chinese National Standard GB/T 1574–2007 using chemical analysis methods, and the results are presented in Table 4. For details on sample preparation, please refer to our previous study [18]. In brief, each sample was ground using a grinder to achieve homogeneity, producing a finely powdered substance sieved through a 125-mesh stainless steel sieve. Subsequently, the obtained samples were put into a loft drier and held at 105 °C for 24 h of air drying to ensure complete drying. This was followed by a 6-h placement in an air-conditioned room to achieve moisture equilibrium. The dried samples were pelletized for analysis using the same method as described in the previous section.

2.2. LIBS measurement

Detailed information on the LIBS measurement system used in this research can be found in our previous study [19]. Briefly, as shown in Fig. 1, the analysis samples were placed on an X-Y-Z motorized platform during LIBS measurements. By adjusting the platform, the laser with a pulse duration of 10 ns was focused 2 mm below the sample surface, where the plasma was generated upon interaction with the laser in atmospheric conditions. A spectrometer was used to collect the light emitted by the plasma, and the gate width of the spectrometer was set to 1.05 ms. To ensure representative spectral information, spectra were collected from 15 different ablating positions of biomass pellets by moving the platform and ablating each position 20 times continuously, i.e., a total of 300 spectra were collected for each sample. According to our previous research [16], the optimal improvement in signal repeatability is achieved when the number of spectra averaged 100. Therefore, the 300 spectra obtained for each sample were divided into three groups (each comprising 100 spectra) for averaging, and the final representation of the spectrum for each sample was the average of these three groups. Moreover, in the pre-experiment, the experimental parameters are optimized using the indicators of peak signal-to-noise ratio, and relative standard deviation of the characteristic emission lines (C, H, O,

Table 4
Reference values of K content in solid biomass fuel samples.

Sample number	K content (%)	Sample number	K content (%)
#1	0.320	#8	0.127
#2	0.190	#9	0.118
#3	0.314	#10	0.402
#4	0.191	#11	0.491
#5	0.066	#12	0.206
#6	0.414	#13	0.151
#7	0.238		

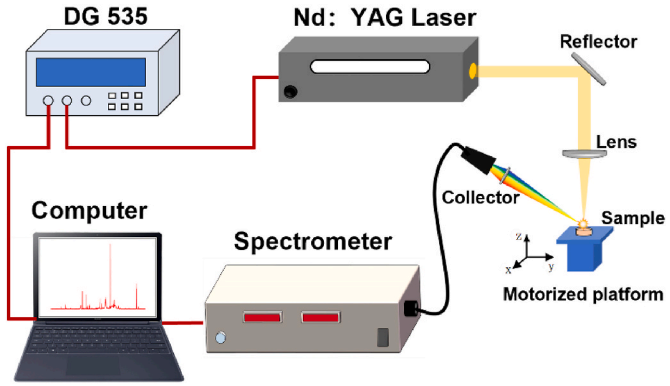

Fig. 1. Diagram of the LIBS measurement system.

and K). Finally, the laser energy and delay time were set as 70 mJ and 1.0 μs, respectively.

2.3. Data processing and analysis

2.3.1. Calibration model

The univariate calibration model is widely applied in LIBS analysis to quantitatively determine elements [33,34]. Based on the fundamental optical physics principle, the characteristic spectral line intensity of the analyzed element is proportional to its corresponding concentration in the sample. However, the univariate calibration model does not account for factors such as matrix effects during the actual measurement process. Consequently, when the sample matrix is complex, the analysis results are often poor. However, this implies that by evaluating the performance of the univariate model provides a direct indication to compare the extent of matrix effects caused by different sample properties. Therefore, we utilized the Scheibe-Lomakin formula [35], the most commonly employed direct calibration method, to establish a univariate equation correlating the intensity of the K 776.49 nm spectral line with the corresponding elemental content.

$$I = aC^b \tag{1}$$

Where I represent the spectral intensity of the characteristic line of the analyte, C denotes the concentration of the analyte, a is the regression coefficient, and b is the self-absorption coefficient, typically assumed to be 1.

Compared to univariate calibration curves, multivariate calibration models can consider more spectral information, compensating for the impact of matrix effects, thereby considerably improving the measurement accuracy. Multiple linear regression (MLR) and partial least square (PLS) is a commonly used multivariate linear regression models in LIBS quantitative analysis. In this study, the MLR and PLS model was employed to establish a quantitative model for K in biomass fuel pellets. Detailed principles regarding those models can be found in the literature [36,37]. Moreover, to overcome significant prediction errors caused by signal uncertainty. We evaluated the performance of three commonly used normalization methods (C-internal standardization, total intensity normalization, and standard normal variate) in processing the raw spectral data. The principles of these three methods are described in detail in the [38]. In this study, a self-programmed MATLAB (MathWorks, 2023) program performed all pre-processing and quantitative analyses of spectral data.

2.3.2. Evaluation indexes of the models

The relative standard deviation (RSD) of spectral signal responses among multiple samples at the same K content was employed to assess the extent of the chemical matrix effect. The determination coefficient (R^2) indicates the goodness of fit of a regression model. The root means square error of prediction (RMSEP), with a lower value indicating higher prediction accuracy. The average standard deviation (ASD), is used to evaluate the repeatability of the model results, with lower values indicating better reproducibility. Their expressions are as follows [39]:

$$RSD = \frac{\sqrt{\frac{\sum_{i=1}^{b}(x_i - \bar{x})^2}{b-1}}}{\bar{x}} \times 100\% \tag{2}$$

$$R^2 = 1 - \frac{\sum_{i=1}^{n}(y_i - \hat{y})^2}{\sum_{i=1}^{n}(y_i - \bar{y})^2} \tag{3}$$

$$RMSEP = \sqrt{\frac{\sum_{i=1}^{m}(y_i - \hat{y})^2}{m}} \tag{4}$$

$$ASD = \frac{\sum_{i=1}^{m}(z_i - \bar{z})}{m} \tag{5}$$

Where b is the number of a set of measurement samples, x_i is the K 776.49 nm spectral intensity of sample *i*, and $\bar{x}$ is the average value of x_i over b samples; n, m denotes the number of the calibration set of samples and the number of the validation set of samples, respectively; y_i, $\hat{y}$ is the reference and predicted values of K contents in biomass, respectively; $\bar{y}$ is the average value of y_i over m samples; z_i represents the standard deviation (SD) value of the predicted value of the validation set sample, and $\bar{z}$ represents the average of z_i over m samples.

3. Results and discussion

3.1. Effects of chemical forms of K on LIBS

3.1.1. Spectral characterization

In this section, the analysis of K spectral lines in 36 cellulose samples was conducted. Based on the database given by the National Institute of Standards and Technology (NIST), the K 766.48 nm spectral line was selected for analysis. Fig. 2a illustrates the spectral intensity measured by LIBS for four different samples of K chemical forms. It can be observed that the spectral intensities of the four samples are not consistent despite being at the same K content. The inconsistency in the spectral signal response among different samples, indicating the influence of chemical matrix effects, was explicitly characterized by the RSD values of K 766.48 nm intensity. As shown in Fig. 2b, the RSD of the K 766.48 nm intensity for different K chemical forms at each content ranged from 1.49 % to 6.5 %. However, this inconsistency in spectral signal response did not exhibit a clear correlation with the chemical forms of K. When ablating the material with a laser, it first destroyed the molecular structure of the analyte. Currently, the chemical bond between the atoms is broken. After the atoms are freed from the bond, their outer electrons transition between the energy levels to radiate the spectral lines representing the corresponding elements [8]. This implies that if the different chemical forms of elements in the sample are the cause of chemical matrix effects in LIBS measurements, the results should show that, at the same content, the maximum and minimum spectral intensities come from samples with specific chemical forms of potassium, respectively. Therefore, the major causes of the inconsistency in the spectral response of the four samples still need to be explored.

In further investigations, considering the influence of laser energy fluctuations on spectral signal intensity, the laser pulse energy was recorded 20 times during the experimental, and its RSD value was calculated (Fig. 2b). It was observed that the inconsistency in spectral signal response among different samples was comparable to the laser energy fluctuation level of 2.3 %. These results show that the chemical matrix effects manifested by various chemical forms of K in the LIBS measurement process are not highly significant. The inconsistency of the spectral signals is mainly caused by the laser energy fluctuations.

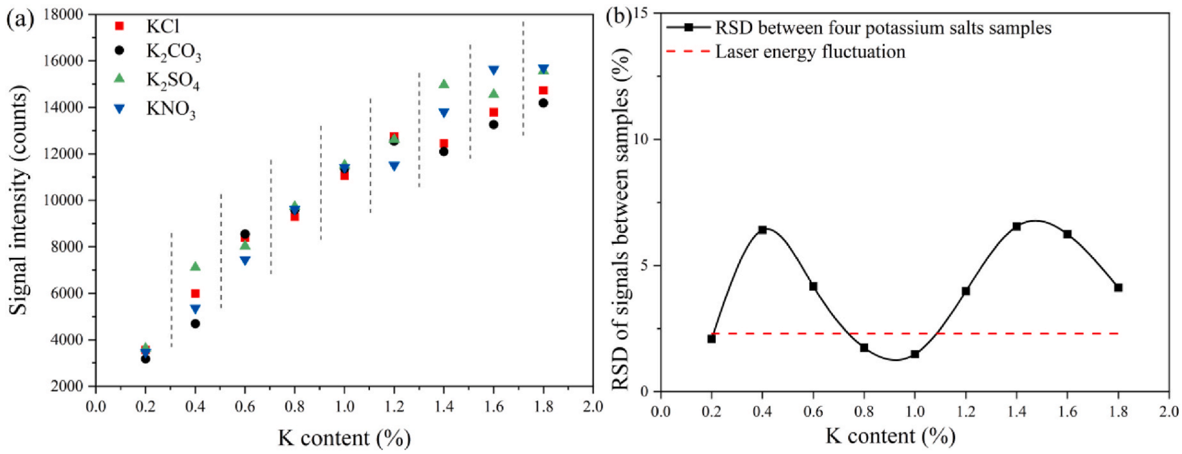

Fig. 2. Four K salts were impregnated in water-washed cellulose as samples. (a) The spectral line intensity of K 766.48 nm for the four samples at different K content. (b) Comparison of LIBS signal response inconsistent and laser pulse-to-pulse energy fluctuation of four samples. (The signal inconsistent is characterized by the RSD of the average spectral intensity of K 766.48 nm for four samples).

Similarly, as argued in the study by Ref. [30], in LIBS measurements of biochar matrix, the effect of differences in the chemical form of an element is minor compared to fluctuations in the laser energy.

3.1.2. Quantitative analysis

Establishing the univariate calibration model to assess the impact of different chemical forms of K on LIBS quantitative analysis. Samples with K content of 0.8 % and 1.6 % were selected as the prediction set, while the remaining samples with seven different concentrations served as the calibration set. The analysis results for each of the four types of samples are presented in Table 5. The R^2 of the three types of samples (except for K_2CO_3) was above 0.93, the RMSEP of the predicted K content of the four samples ranged from 0.69 to 1.01 %, and the SD of the predicted values for the K content of the repeated measurements ranged from 0.05 % to 0.46 %. Furthermore, the univariate calibration model was performed for all 36 samples of the four K different chemical forms together. The results are shown in Fig. 3. The overall sample quantitative results closely resemble the results obtained individually for each type of sample, with an R^2 of 0.933, an RMSEP of 0.69 %, and an ASD of 0.16 %. Further, considering the inconsistency of spectral response in 2.1.1. the total spectral intensity normalization method was used to process the averaged spectral data before establishing the calibration curve. The results are shown in Fig. 3b, where the R^2 is improved to 0.942, the RMSEP and ASD are decreased to 0.139 % and 0.007 %, respectively, and the prediction accuracy and robustness of the univariate model are significantly improved.

Chemical matrix effects primarily manifest as inconsistencies in spectral signal responses among different samples, further impacting the results of quantitative analysis. Compared to multivariate models or machine learning algorithms, the performance of univariate models provides a more intuitive representation of the impact of matrix effects [40]. In this section, the individual calibration curves for each sample type showed minimal deviation from their overall calibration curves and prediction performance. Additionally, the accuracy and precision of the general calibration curves significantly improved after reducing spectral fluctuations through spectral intensity normalization. This indicates that in LIBS measurements, the chemical form of the analyte does not induce significant chemical matrix effects. In other words, the spectral signals between biomass samples with different chemical forms of K still exhibit a linear relationship with their corresponding K content.

3.2. Effects of matrix composition of biomass on LIBS

3.2.1. Spectral characterization

In LIBS measurement, the elemental emission intensity is not only related to their content but also depends on the specific chemical properties of the samples. The different chemical forms of elements can result in varied emission intensities, as discussed in the previous section. Moreover, the properties and content of other elements in the sample can also induce corresponding enhancement or attenuation effects on the emission intensity. In our study, we analyzed the spectra characterization of biomass samples with three different compositions under specific potassium forms (KCl), as illustrated in Fig. 4. The spectral signal response of K in the samples at a given content range (0.2%–1.8 %). It can be obviously noticed that the signal intensity of the K 766.48 nm spectral line of the lignin sample (overall spectral intensity range of 8000–16000) is much higher than that of the cellulose and biomass samples (overall spectral intensity range of 3900–14000) at the same content, displaying a serious chemical matrix effect. Further, Fig. 4b specifically quantifies the inconsistency of the spectral signal response of samples. The signal intensity RSD values among the three types of samples at the same content ranged from 10 % to 43 %, with an average of 19.58 %, which fluctuated at a level much higher than that of the laser energy (2.3 %). Suggesting that the different composition of the samples led to different laser ablation behaviors, which, in consequence, resulted in different spectra.

Table 5
The calibrations and predicted results for four different chemical forms of K samples.

calibration curve	R^2	Predicted value of K content (%)								RMSEP (%)
		KCl(0.80% K)	KCl(1.60% K)	K_2CO_3(0.80% K)	K_2CO_3(1.60% K)	K_2SO_4(0.80% K)	K_2SO_4(1.60% K)	KNO_3(0.80% K)	KNO_3(1.60% K)	
KCl	0.932	0.86(0.12)	1.52(0.13)	0.91(0.18)	1.44(0.05)	0.93(0.24)	1.63(0.06)	0.91(0.06)	1.79(0.31)	0.69
K_2CO_3	0.884	0.91(0.12)	1.56(0.13)	0.95(0.17)	1.48(0.06)	0.97(0.21)	1.67(0.06)	0.96(0.06)	1.82(0.40)	1.01
K_2SO_4	0.945	0.78(0.11)	1.38(0.12)	0.82(0.16)	1.31(0.05)	0.84(0.22)	1.48(0.05)	0.82(0.05)	1.63(0.46)	0.90
KNO_3	0.950	0.87(0.10)	1.45(0.11)	0.91(0.16)	1.38(0.05)	0.93(0.21)	1.55(0.05)	0.91(0.06)	1.69(0.45)	0.79

Notes: The values in brackets represent the SD of the predicted K content from repeated measurements.

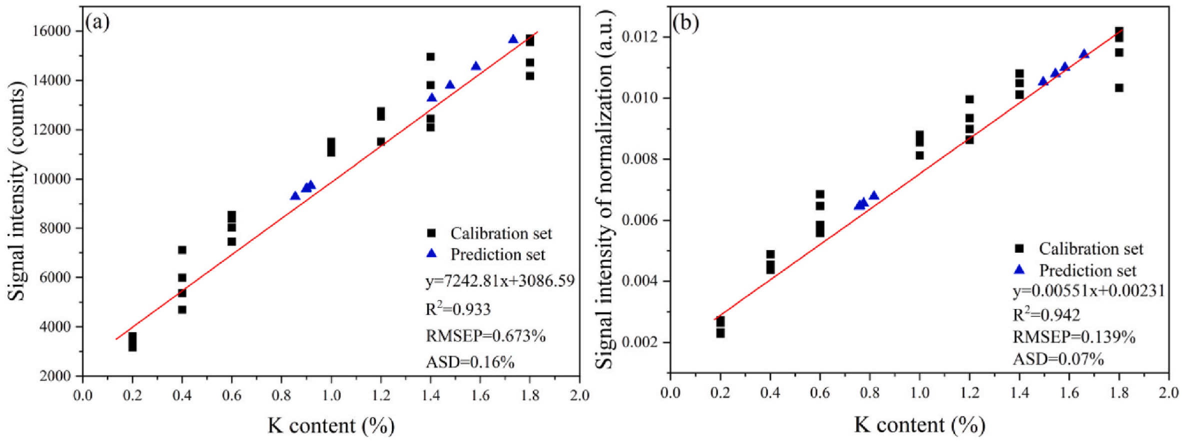

Fig. 3. Before (a) and after (b) normalization, the Calibration curves and prediction result for the element K in biomass samples performed with LIBS.

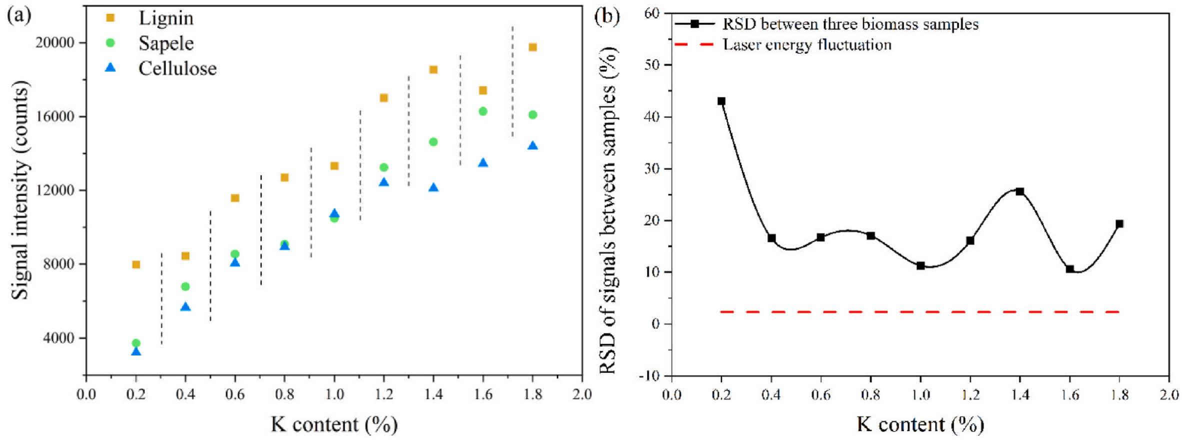

Fig. 4. Impregnation of KCl in washed three types of biomasses matrix as samples. (a) The signal intensity of K 766.48 nm in the three samples. (b) There was an inconsistency of LIBS signal response among the three samples and energy fluctuation between laser pulses. (The signal inconsistent is characterized by the RSD of the average spectral intensity of K I 766.48 nm for different samples).

It is noteworthy that the differences in the spectral response of K exhibit a high correlation with the types of matrixes. Across all ranges of K content, the K line intensity is highest in the lignin sample, followed by the Sapele, slightly higher than cellulose (Fig. 4a). Proximate analysis of the composition for the three types of matrices reveals that cellulose has the highest volatile content at 86.46 %, followed by biomass at 80.02 %, and lignin with the least volatile content at only 60.43 % (Table 4). Studies [41] indicate that the presence of volatile composition inhibits the emission intensity of mineral elements. Specifically, for carbon-based solid fuels such as biomass and coal, the presence of volatile substances makes them more easily ignitable in the interaction with lasers compared to other solid materials (metals, rocks, soils, etc.) [42, 43]. In this process, the laser pulse's pyrolysis and the evaporation, dissociation, and ionization of volatiles consume significant energy, thereby suppressing the excitation of other mineral elements. Additionally, the ash content plays an enhancing role in the emission signals of metals and mineral elements [44]. This is attributed to the presence of numerous metal elements, such as Si, Al, Fe, Ca, Mg, etc., in ash materials. These elements are easily excited due to their low ionization energies. Under the same laser energy, the substantial excitation of these metal elements with low ionization energy leads to an increase in plasma temperature, thereby promoting the excitation of spectral lines of other elements in the sample. As shown in Fig. 5, among the three matrices, lignin exhibits the highest metal element types. Similarly, its approximate analysis indicates an ash content of 14.75 %, which is more than twice as high as the other two matrices (Table 4). Thus, these results suggest that due to the inhibitory and enhancing effects of volatile and ash content on K emission signals, lignin shows the strongest K line intensity, while cellulose and lignin are relatively similar. This also indicates that in LIBS analysis of biomass fuels, compositional differences, rather than the chemical forms of the elements under investigation, are the main sources of chemical matrix effects.

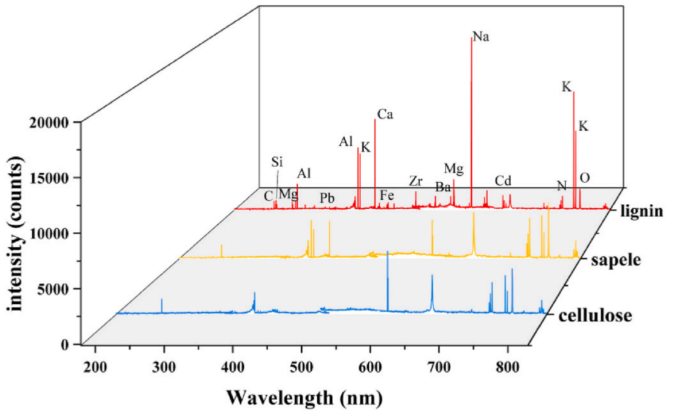

Fig. 5. The average LIBS spectra of lignin, sapele, and cellulose biomass impregnated with 1.8 % KCl.

3.2.2. Quantitative analysis

Univariate analysis of the K content for different samples is shown in Fig. 6. The calibration curves for K content within each individual sample exhibit satisfactory fitting results, with R^2 values all exceeding 0.941. However, the combined calibration and prediction results for the three types of samples are far from ideal, with R^2 is 0.719 and a high RMSPE is 2.12 %. This suggests that the influence of composition present in samples results in a non-linear relationship between LIBS spectral signals and the corresponding analyte concentrations. Consequently, the fitting performance of univariate models deteriorates, impeding the analytical capability of LIBS. When compared to the results in Section 2.2.2, it is evident that, between the two types of matrix differences involving the analyte's chemical form and the matrix composition of the samples, the latter exerts a more dominant impact on the quantitative analysis by LIBS, and serves as the major source of the chemical matrix effect.

3.3. K LIBS detection on solid biomass fuel

3.3.1. Univariate calibration model

Through the above results, we can conclude that in biomass samples, the composition of the sample introduces a non-linear relationship in LIBS spectra, significantly affecting its analytical performance. As shown in Fig. 7, are the K quantitative results of Univariate calibration based on the intensity of K 766.49 nm, with samples #4, #7 and #12 selected as the prediction set. For the 13 samples of biomass fuel pellets, the univariate calibration model exhibits an inferior fit, with 0.131 of R^2, the RMSEP and ASD are 0.78 % and 0.29 %, respectively, which were too wide errors for the range of K contents in biomass fuel pellets. Moreover, the performance of the univariate model is significantly degraded compared to the standard biomass samples analyzed in Sections 3.1 and 3.2. These results indicated that the complex matrix component of biomass fuels leads to the ineffectiveness of the univariate strategies. In contrast to biomass samples used in the experiment, real solid biomass fuels are typically formed by compressing agricultural and forestry waste whose composition and element chemical form is more complex and variable [45]. This suggests that the chemical matrix effect needs further consideration in K LIBS detection of solid biomass fuel.

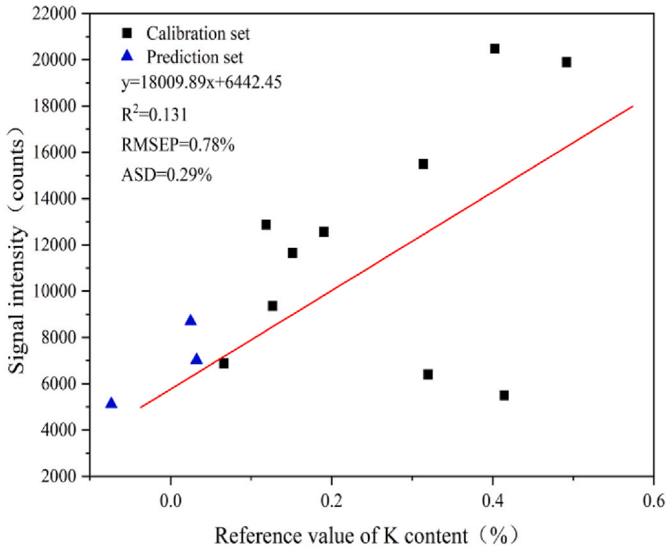

Fig. 7. Calibration and prediction results for solid biomass fuel sample with univariate model.

3.3.2. Correction for chemical matrix effect

The multiple variables for calibration is an effective approach to minimize the chemical matrix effect in LIBS and improve the modeling performance when matrix-related spectral information should be introduced [46]. However, most of those methods ignore the background knowledge of the sample as they are dependent on data-driven. This may result in noise overfitting, potentially compromising the accuracy of measurements for samples outside the calibration sample set's matrix [47]. Therefore, we adopted a knowledge-based regression strategy to incorporate the identified major factors affecting chemical matrix effects in biomass as a priori knowledge into the regression model, thus further improving the model performance.

Firstly, the chemical matrix effect in the quantitative analysis of K for biomass fuels was corrected by employing a MLR model. The results are presented in Fig. 8. Considering the impact of ash content on the K spectral intensity, we constructed a multivariate regression model using the spectral intensities of Mg 280.33 nm, Si 288.13 nm, Al 309.23 nm, Fe 373.93 nm, Ca 393.58 nm, Na 589.00 nm, and K 766.49 nm as independent variables. Compared to the univariate model in Fig. 8, the R^2, RMSEP, and ASD improved to 0.742, 0.092 %, and 0.105 %, respectively. This indicates that introducing ash-related information can correct chemical matrix effects to some extent and improve quantitative accuracy. However, it still falls short compared to the univariate quantitative results (section 3.2) for Samples from the same matrix. The reason might be that, as previously analyzed, volatile matter in biomass is also a major source of chemical matrix effects, affecting the spectral intensity of K. Volatile matter [48] mainly includes combustible gases such as H, CO, hydrocarbons, and non-combustible gases like CO_2 and water vapors. This means that compensating for chemical matrix effects by selecting specific spectral features to characterize the volatile fraction information is difficult. Hence, simultaneously introducing ash and

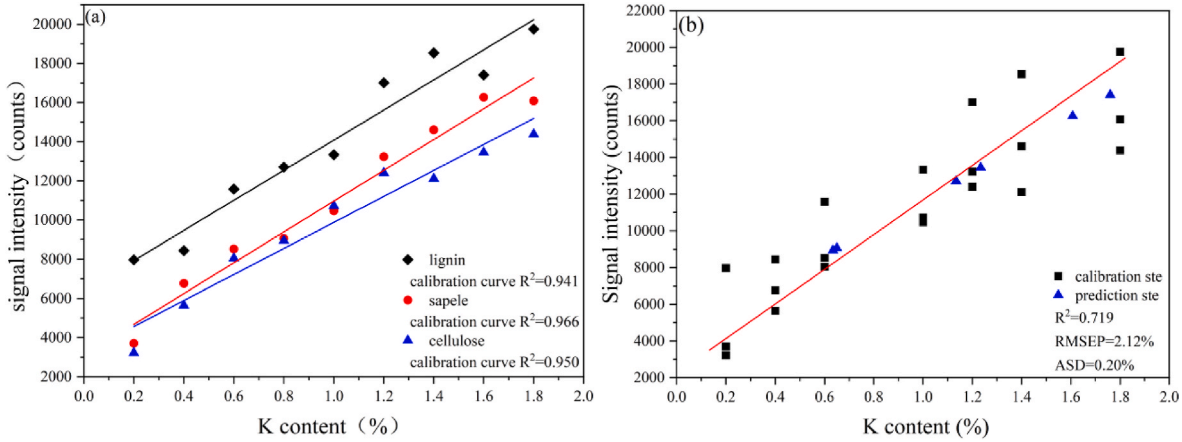

Fig. 6. (a) Calibration results for each of the three types of biomass samples; (b) Calibration and prediction results for the three types of samples together.

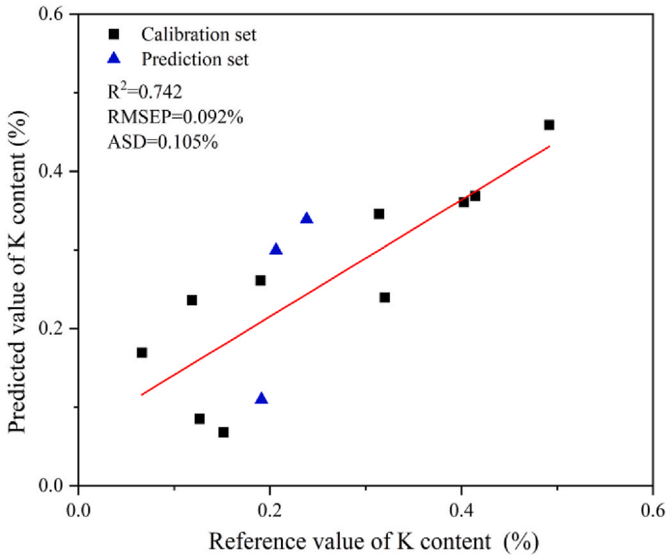

Fig. 8. Quantification results of K content for solid biomass fuel sample with MLR.

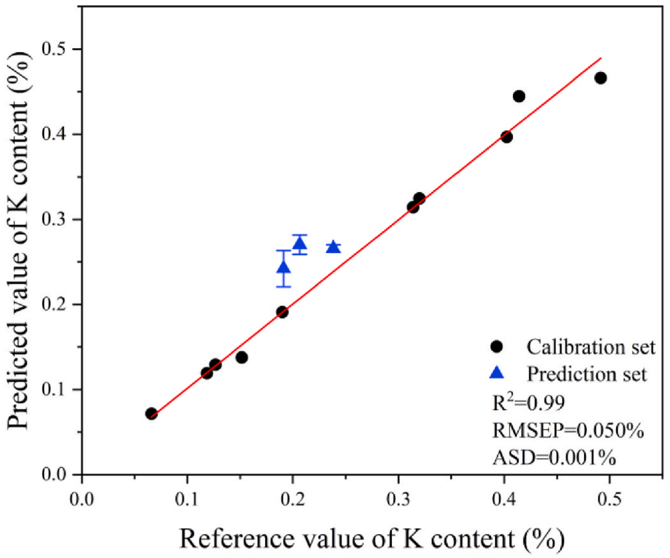

Fig. 9. Quantitative analysis results of K content for real biomass fuel sample used PLS model with variable selection.

volatile fraction information into the model becomes important.

Although it is challenging to correlate volatile matter with specific elemental spectral lines, analyzing the full spectrum containing all biomass information using PLS can effectively reflect the volatile content [19]. Therefore, we carried out proximate analyses to 13 biomasses (see Table S1 in supplementary). And Supplementary Fig. S1 shows the fitting results of biomass fuel volatile content based on PLS. As seen in the figure, the relationship between the volatile content of the 13 biomass fuels and the spectral data is well represented by PLS. The R^2 is 0.952, and the RMSEP is 1.553 %, indicating that PLS can accurately fit the volatile content in biomass fuels. Additionally, by inputting the full spectrum, the information on ash elements is also incorporated into the model, thereby correcting the chemical matrix effects. Although the full spectrum contains sufficient information about the matrix components, it is not an ideal choice for elemental analysis. Including too many variables increases the complexity of the model, reduces analytical accuracy, and raises the risk of overfitting.

Therefore, a weighted PLS filtering method [49,50] was utilized to make a selection of variables, before performing the PLS regression. The procedure is as follows: (1) The spectral data is processed using SNV and then input into the PLS model. Based on the principle of minimizing the root mean square error of cross-validation (RMSECV), leave-one-out cross-validation (LOOCV) is used to select the optimal number of principal components and corresponding model for PLS; (2) After obtaining the PLS model, variables are filtered using the weight coefficient of the K 769.71 nm spectral line as the threshold, resulting in a new spectral matrix containing 168 variables; (3) Using the new spectral matrix, PLS regression was performed again (the optimal principal components was 2), ultimately resulting in the quantitative model for K content in biomass fuel. Details of the weight threshold settings and the choice of data processing methods can be found in the Supplementary Material. It is worth noting that the above method reduced the number of model input variables from 8192 full-spectrum variables to 168 variables, significantly decreasing the model's complexity and making it more efficient. The results are shown in Fig. 9, with error bars representing the ASD values from three LIBS measurements for each sample. The model achieved an R^2 of 0.99, with an RMSEP of 0.050 % for the prediction set samples. Although the PLS model using full-spectrum input had slightly better prediction accuracy (see Fig. S3 in supplementary), reducing the input variables greatly improved the model's stability, with ASD decreasing from 0.030 % to 0.001 %. Additionally, incorporating known chemical knowledge increased the model's interpretability, making it more extendable and helping to avoid overfitting.

4. Conclusion

In this study, a series of samples were configured for LIBS experiments to assess different sources of chemical matrix effects in biomass. The results indicate that, compared to the various chemical forms of the analyte, the compositional differences in the biomass matrix have a more significant impact on spectral responses and quantitative analysis. Under the same contents of K, the RSD values of spectral signals between three different biomass samples ranged from 10 % to 43 %, and the R^2 of the univariate calibration curves of K content was only 0.719, which was subjected to a strong chemical matrix effect. Subsequently, further analysis of the composition of the samples revealed that for lignin with high ash content and low volatile matter content, the spectral response signals were the strongest, attributed to the effect of volatiles and ash on emission intensity suppression and enhancement.

Finally, LIBS was used to measure biomass fuel pellets in real power plants. Based on the findings of our study above, PLS regression was employed to mitigate the impact of chemical matrix effects, using the select specific spectrum as input variables. Various data processing methods were compared, leading to the establishment of quantitative models for K contents. The optimal R^2, RMSEP, and ASD were 0.99, 0.050 %, and 0.001 %, respectively, validating the feasibility of LIBS for rapidly analyzing K content in biomass fuel. However, the small number of samples available to us for analysis may pose certain limitations.

Therefore, the next step of the work will be to obtain more biomass fuel samples and investigate how to improve the interpretability and accuracy of the model. In addition, we recommend paying particular attention to the volatile matter and ash content in biomass fuels to overcome chemical matrix effects better. Further classification based on volatile matter and ash content, along with the use of multivariate models or non-linear machine learning algorithms, is suggested to analyze alkali metal elements in biomass fuels.

CRediT authorship contribution statement

Chengjun Li: Writing – original draft, Visualization, Investigation, Formal analysis. **Zhimin Lu:** Writing – review & editing, Resources, Methodology, Conceptualization. **Jinzheng Chen:** Investigation. **Ziyu Yu:** Software. **Qi Yang:** Writing – review & editing, Formal analysis. **Huaiqing Qin:** Investigation, Data curation. **Xiwen Xing:** Supervision,

Resources. **Qingxiang Ma:** Writing – review & editing. **Shunchun Yao:** Writing – review & editing, Supervision, Project administration, Funding acquisition.

Declaration of competing interest

The authors declare that they have no known competing financial interests or personal relationships that could have appeared to influence the work reported in this paper.

Acknowledgments

This research was financially supported by the Nature Science Foundation of Guangdong Province (2022A1515010741), Natural Science Foundation of Guangdong Province for Distinguished Youth (No. 2021B1515020071), The Fundamental Research Funds for the Central Universities (No. 2023ZYGXZR090), Foundation of State Key Laboratory of High efficiency Utilization of Coal and Green Chemical Engineering (No.2022-K72).

Appendix A. Supplementary data

Supplementary data to this article can be found online at https://doi.org/10.1016/j.aca.2024.343568.

Data availability

Data will be made available on request.

References

[1] Yan Xu, Kun Yang, Jiahui Zhou, Guohao Zhao, Coal-biomass Co-firing power generation technology: current status, challenges and policy implications, Sustainability 12 (2020) 3692, https://doi.org/10.3390/su12093692.

[2] Yanqing Niu, Houzhang Tan, Shi'en Hui, Ash-related issues during biomass combustion: Alkali-induced slagging, silicate melt-induced slagging (ash fusion), agglomeration, corrosion, ash utilization, and related countermeasures, Prog. Energy Combust. Sci. 52 (2016) 1–61, https://doi.org/10.1016/j.pecs.2015.09.003.

[3] Q.H. Li, Y.G. Zhang, A.H. Meng, L. Li, G.X. Li, Study on ash fusion temperature using original and simulated biomass ashes, Fuel Process. Technol. 107 (2013) 107–112, https://doi.org/10.1016/j.fuproc.2012.08.012.

[4] Y. Niu, H. Tan, L. Ma, M. Pourkashanian, Z. Liu, Y. Liu, X. Wang, H. Liu, T. Xu, Slagging characteristics on the superheaters of a 12 MW biomass-fired boiler, Energy Fuels 24 (2010) 5222–5227, https://doi.org/10.1021/ef1008055.

[5] H. Uvegi, P. Chaunsali, B. Traynor, E. Olivetti, Reactivity of industrial wastes as measured through ICP-OES: a case study on siliceous Indian biomass ash, J. Am. Ceram. Soc. 102 (2019) 7678–7688, https://doi.org/10.1111/jace.16628.

[6] T. Khazraie Shoulaifar, N. DeMartini, M. Zevenhoven, F. Verhoeff, J. Kiel, M. Hupa, Ash-forming matter in torrefied birch wood: changes in chemical association, Energy Fuels 27 (2013) 5684–5690, https://doi.org/10.1021/ef4005175.

[7] D.M. Le, H.R. Sørensen, A.S. Meyer, Elemental analysis of various biomass solid fractions in biorefineries by X-ray fluorescence spectrometry, Biomass Bioenergy 97 (2017) 70–76, https://doi.org/10.1016/j.biombioe.2016.12.018.

[8] Front Matter, in: Handbook of Laser-Induced Breakdown Spectroscopy, John Wiley & Sons Ltd, Oxford, UK, 2013, pp. i–xvii, https://doi.org/10.1002/9781118567371.fmatter.

[9] Gardette Vincent, Vincent Motto-Ros, César Alvarez-Llamas, Lucie Sancey, Ludovic Duponchel, Benoit Busser, Laser-induced breakdown spectroscopy imaging for material and biomedical applications: recent advances and future perspectives, Anal. Chem. 95 (2023) 49–69, https://doi.org/10.1021/acs.analchem.2c04910.

[10] Meirong Dong, Junbin Cai, Hongchuan Liu, Junchang Xiong, Gangfu Rao, Shunchun Yao, Jidong Lu, A review of laser-induced breakdown spectroscopy and spontaneous emission techniques in monitoring thermal conversion of fuels, Spectrochim. Acta, Part B 210 (2023) 106807, https://doi.org/10.1016/j.sab.2023.106807.

[11] Wubin Weng, Marcus Aldén, Zhongshan Li, Insight into KOH and KCl release behavior of burning wood and straw pellets using quantitative in situ optical measurements, Proc. Combust. Inst. 39 (2023) 3239–3248, https://doi.org/10.1016/j.proci.2022.07.079.

[12] Oris Chansa, Zhongyang Luo, Eric G. Eddings, Chunjiang Yu, Determination of alkali release during oxyfuel co-combustion of biomass and coal using laser-induced breakdown spectroscopy, Fuel 289 (2021) 119658, https://doi.org/10.1016/j.fuel.2020.119658.

[13] Haibo Zhao, M.A. Wakil, Jan Viljanen, Qiang Song, Qiang Yao, C.W. Kwong, Zeyad T. Alwahabi, In situ measurement of potassium release during biomass combustion using laser-induced breakdown spectroscopy: effect of silicate on potassium release, Energy Fuels 34 (2020) 3262–3271, https://doi.org/10.1021/acs.energyfuels.9b03966.

[14] Yingzu Liu, Kaidi Wan, Yong He, Zhihua Wang, Jun Xia, Kefa Cen, Experimental study of potassium release during biomass-pellet combustion and its interaction with inhibitive additives, Fuel 260 (2020) 116346, https://doi.org/10.1016/j.fuel.2019.116346.

[15] Xiaodan Liu, Xuping Feng, Lingxia Huang, Yong He, Rapid determination of wood and rice husk pellets' proximate analysis and heating value, Energies 13 (2020) 3741, https://doi.org/10.3390/en13143741.

[16] Zhimin Lu, Xiaoxuan Chen, Shunchun Yao, Huaiqing Qin, Lifeng Zhang, Xiayang Yao, Ziyu Yu, Jidong Lu, Feasibility study of gross calorific value, carbon content, volatile matter content and ash content of solid biomass fuel using laser-induced breakdown spectroscopy, Fuel 258 (2019) 116150, https://doi.org/10.1016/j.fuel.2019.116150.

[17] Xiaodan Liu, Xuping Feng, Yong He, Rapid discrimination of the categories of the biomass pellets using laser-induced breakdown spectroscopy, Renew. Energy 143 (2019) 176–182, https://doi.org/10.1016/j.renene.2019.04.137.

[18] Zhimin Lu, Xiaoxuan Chen, Yuan Jiang, Xin Li, Jinzheng Chen, Yuesheng Li, Weiye Lu, Jidong Lu, Shunchun Yao, Application of laser induced breakdown spectroscopy for direct and quick determination of fuel property of woody biomass pellets, Renew. Energy 164 (2021) 1204–1214, https://doi.org/10.1016/j.renene.2020.10.112.

[19] Yuan Jiang, Zhimin Lu, Xiaoxuan Chen, Ziyu Yu, Huaiqing Qin, Jinzheng Chen, Jidong Lu, Shunchun Yao, Optimizing the quantitative analysis of solid biomass fuel properties using laser induced breakdown spectroscopy (LIBS) coupled with a kernel partial least squares (KPLS) model, Anal. Methods 13 (2021) 5467–5477, https://doi.org/10.1039/D1AY01639C.

[20] V. Palleschi (Ed.), Front Matter, in: Chemometrics and Numerical Methods in LIBS, first ed., Wiley, 2022 https://doi.org/10.1002/9781119759614.fmatter.

[21] S. Yao, J. Zhao, J. Xu, Z. Lu, J. Lu, Optimizing the binder percentage to reduce matrix effects for the LIBS analysis of carbon in coal, J. Anal. At. Spectrom. 32 (2017) 766–772, https://doi.org/10.1039/C6JA00458J.

[22] C. Li, Z. Ding, T. Zhang, Z. Bao, M. Guo, M. Wang, Y. Bi, Research on improving the accuracy of laser-induced breakdown spectroscopy analysis by considering plasma attenuation rate characteristics, Anal. Chim. Acta 1287 (2024) 342065, https://doi.org/10.1016/j.aca.2023.342065.

[23] Q. Wang, J. Xiao, Y. Li, Y. Lu, J. Guo, Y. Tian, L. Ren, Mid-level data fusion of Raman spectroscopy and laser-induced breakdown spectroscopy: improving ores identification accuracy, Anal. Chim. Acta 1240 (2023) 340772, https://doi.org/10.1016/j.aca.2022.340772.

[24] Lu-Ning Li, Xiang-Feng Liu, Fan Yang, Wei-Ming Xu, Jian-Yu Wang, Rong Shu, A review of artificial neural network based chemometrics applied in laser-induced breakdown spectroscopy analysis, Spectrochim. Acta B Atom Spectrosc. 180 (2021) 106183, https://doi.org/10.1016/j.sab.2021.106183.

[25] W. Song, M.S. Afgan, Y.-H. Yun, H. Wang, J. Cui, W. Gu, Z. Hou, Z. Wang, Spectral knowledge-based regression for laser-induced breakdown spectroscopy quantitative analysis, Expert Syst. Appl. 205 (2022) 117756, https://doi.org/10.1016/j.eswa.2022.117756.

[26] J. Long, W. Song, Z. Hou, Z. Wang, A data selection method for matrix effects and uncertainty reduction for laser-induced breakdown spectroscopy, Plasma Sci. Technol. 25 (2023) 075501, https://doi.org/10.1088/2058-6272/acb6dd.

[27] Sara Sánchez-Esteva, Maria Knadel, Rodrigo Labouriau, Gitte H. Rubæk, Goswin Heckrath, Total phosphorus determination in soils using laser-induced breakdown spectroscopy: evaluating different sources of matrix effects, Appl. Spectrosc. 75 (2021) 22–33, https://doi.org/10.1177/0003702820949560.

[28] Meirong Dong, Fa-Sheng Luo, Min Huang, Shi-Shi Li, Wei-Hao Zhao, Ji-Dong Lu, Study on the ignition characteristics and alkali release of single coal particles with additional different forms of potassium, Fuel Process. Technol. 203 (2020) 106385, https://doi.org/10.1016/j.fuproc.2020.106385.

[29] S. Grünberger, V. Ehrentraut, S. Eschlböck-Fuchs, J. Hofstadler, A. Pissenberger, J. D. Pedarnig, Overcoming the matrix effect in the element analysis of steel: laser ablation-spark discharge-optical emission spectroscopy (LA-SD-OES) and Laser-induced breakdown spectroscopy (LIBS), Anal. Chim. Acta 1251 (2023) 341005, https://doi.org/10.1016/j.aca.2023.341005.

[30] Mei Guo, Rongguang Zhu, Lixin Zhang, Ruoyu Zhang, Guangqun Huang, Hongwei Duan, Quantitative detection of chromium pollution in biochar based on matrix effect classification regression model, Molecules 26 (2021) 2069, https://doi.org/10.3390/molecules26072069.

[31] S.V. Vassilev, C.G. Vassileva, V.S. Vassilev, Advantages and disadvantages of composition and properties of biomass in comparison with coal: an overview, Fuel 158 (2015) 330–350, https://doi.org/10.1016/j.fuel.2015.05.050.

[32] L. Deng, T. Zhang, D. Che, Effect of water washing on fuel properties, pyrolysis and combustion characteristics, and ash fusibility of biomass, Fuel Process. Technol. 106 (2013) 712–720, https://doi.org/10.1016/j.fuproc.2012.10.006.

[33] J. Chen, W. Yan, L. Kang, B. Lu, K. Liu, X. Li, Accuracy improvement of laser-induced breakdown spectroscopy coal analysis by hybrid transfer learning, Anal. Methods 15 (2023) 5157–5165, https://doi.org/10.1039/D3AY01380D.

[34] M. Huang, H. Xu, High accuracy determination of copper in copper concentrate with double genetic algorithm and partial least square in laser-induced breakdown spectroscopy, Opt Express 28 (2020) 2142, https://doi.org/10.1364/OE.381582.

[35] É.Ya Ogneva, YaD. Raikhbaum, B.R. Ognev, An interpretation of lomakin-sheibe formula, J. Appl. Spectrosc. 17 (1972) 1530–1533, https://doi.org/10.1007/BF00618947.

[36] L.S. Aiken, S.G. West, R.R. Reno, Multiple Regression: Testing and Interpreting Interactions, SAGE, 1991.

[37] S. Yao, H. Qin, Q. Wang, Z. Lu, X. Yao, Z. Yu, X. Chen, L. Zhang, J. Lu, Optimizing analysis of coal property using laser-induced breakdown and near-infrared reflectance spectroscopies, Spectrochim. Acta Mol. Biomol. Spectrosc. 239 (2020) 118492, https://doi.org/10.1016/j.saa.2020.118492.

[38] J. Guezenoc, A. Gallet-Budynek, B. Bousquet, Critical review and advices on spectral-based normalization methods for LIBS quantitative analysis, Spectrochim. Acta B Atom Spectrosc. 160 (2019) 105688, https://doi.org/10.1016/j.sab.2019.105688.

[39] J.-B. Sirven, B. Bousquet, L. Canioni, L. Sarger, Laser-induced breakdown spectroscopy of composite samples: comparison of advanced chemometrics methods, Anal. Chem. 78 (2006) 1462–1469, https://doi.org/10.1021/ac051721p.

[40] C. Zhang, W. Song, Z. Hou, Z. Wang, Improving quantitative analysis of cement elements in laser-induced breakdown spectroscopy through combining matrix matching with regression, J. Anal. At. Spectrom. 38 (2023) 2554–2561, https://doi.org/10.1039/D3JA00306J.

[41] Shunchun Yao, Jingbo Zhao, Zhenzhen Wang, Yoshihiro Deguchi, Zhimin Lu, Jidong Lu, Analysis of spectral properties for coal with different volatile contents by laser-induced breakdown spectroscopy, Spectrochim. Acta B Atom Spectrosc. 149 (2018) 249–255, 10/grwscz.

[42] B.P. Aduev, D.R. Nurmukhametov, R.Yu Kovalev, YaV. Kraft, A.N. Zaostrovskii, A. V. Gudilin, Z.R. Ismagilov, Spectral-kinetic characteristics of laser ignition of pulverized Brown coal, Opt. Spectrosc. 125 (2018) 293–299, https://doi.org/10.1134/S0030400X18080039.

[43] L. Haas, Reprints available directly from the publisher Photocopying permitted by license only, Review of Education, Pedagogy, and, Cult. Stud. 17 (1995) 1–6, https://doi.org/10.1080/1071441950170102.

[44] Ziyu Yu, Shunchun Yao, Yuan Jiang, Weize Chen, Shuixiu Xu, Huaiqing Qin, Zhimin Lu, Jidong Lu, Comparison of the matrix effect in laser induced breakdown spectroscopy analysis of coal particle flow and coal pellets, J. Anal. At. Spectrom. 36 (2021) 2473–2479, https://doi.org/10.1039/D1JA00223F.

[45] S. Pang, Advances in thermochemical conversion of woody biomass to energy, fuels and chemicals, Biotechnol. Adv. 37 (2019) 589–597, https://doi.org/10.1016/j.biotechadv.2018.11.004.

[46] Z. Hou, Z. Wang, T. Yuan, J. Liu, Z. Li, W. Ni, A hybrid quantification model and its application for coal analysis using laser induced breakdown spectroscopy, J. Anal. At. Spectrom. 31 (2016) 722–736, https://doi.org/10.1039/C5JA00475F.

[47] A. Safi, B. Campanella, E. Grifoni, S. Legnaioli, G. Lorenzetti, S. Pagnotta, F. Poggialini, L. Ripoll-Seguer, M. Hidalgo, V. Palleschi, Multivariate calibration in laser-induced breakdown spectroscopy quantitative analysis: the dangers of a ‘black box’ approach and how to avoid them, Spectrochim. Acta, Part B 144 (2018) 46–54, https://doi.org/10.1016/j.sab.2018.03.007.

[48] M. Dong, J. Lu, S. Yao, J. Li, J. Li, Z. Zhong, W. Lu, Application of LIBS for direct determination of volatile matter content in coal, J. Anal. At. Spectrom. 26 (2011) 2183–2188, https://doi.org/10.1039/C1JA10109A.

[49] A review of variable selection methods in Partial Least Squares Regression, Chemometr. Intell. Lab. Syst. 118 (2012) 62–69, https://doi.org/10.1016/j.chemolab.2012.07.010.

[50] Å. Rinnan, M. Andersson, C. Ridder, S.B. Engelsen, Recursive weighted partial least squares (rPLS): an efficient variable selection method using PLS, J. Chemom. 28 (2014) 439–447, https://doi.org/10.1002/cem.2582.